

All studies published in Gastroenterology are embargoed until 3PM ET of the day they are published as corrected proofs on-line.
 Studies cannot be publicized as accepted manuscripts or uncorrected proofs.

Hepatitis C Virus Infects the Endothelial Cells of the Blood-Brain Barrier

NICOLA F. FLETCHER,* GARRICK K. WILSON,* JACINTA MURRAY,[‡] KE HU,* ANDREW LEWIS,[§] GARY M. REYNOLDS,* ZANIA STAMATAKI,* LUKE W. MEREDITH,* IAN A. ROWE,* GUANGXIANG LUO,^{||} MIGUEL A. LOPEZ-RAMIREZ,[¶] THOMAS F. BAUMERT,[#] BABELLE WEKSLER,** PIERRE-OLIVIER COURAUD,^{††} KWANG SIK KIM,^{§§} IGNACIO A. ROMERO,^{¶¶} CATHERINE JOPLING,[§] SUSAN MORGELLO,[‡] PETER BALFE,* and JANE A. McKEATING*

*Hepatitis C Research Group, Institute for Biomedical Research, University of Birmingham, Birmingham, England; [‡]Department of Pathology, Mount Sinai School of Medicine, New York, New York; [§]School of Pharmacy, University of Nottingham, Nottingham, England; ^{||}Department of Microbiology, Immunology and Molecular Genetics, University of Kentucky, Lexington, Kentucky; [¶]Department of Life Sciences, The Open University, Milton Keynes, England; [#]Université de Strasbourg and Pôle Hépatodigestif, Hôpitaux Universitaires de Strasbourg, Strasbourg, France; ^{**}Weill Cornell Medical College, New York, New York; ^{††}Institut Cochin, CNRS UMR 8104, INSERM Unité 567, Université Paris Descartes, Paris, France; and ^{§§}Division of Infectious Diseases, The Johns Hopkins School of Medicine, Baltimore, Maryland

BACKGROUND & AIMS: Hepatitis C virus (HCV) infection leads to progressive liver disease and is associated with a variety of extrahepatic syndromes, including central nervous system (CNS) abnormalities. However, it is unclear whether such cognitive abnormalities are a function of systemic disease, impaired hepatic function, or virus infection of the CNS. **METHODS:** We measured levels of HCV RNA and expression of the viral entry receptor in brain tissue samples from 10 infected individuals (and 3 uninfected individuals, as controls) and human brain microvascular endothelial cells by using quantitative polymerase chain reaction and immunofluorescence and confocal imaging analyses. HCV pseudoparticles and cell culture-derived HCV were used to study the ability of endothelial cells to support viral entry and replication. **RESULTS:** Using quantitative polymerase chain reaction, we detected HCV RNA in brain tissue of infected individuals at significantly lower levels than in liver samples. Brain microvascular endothelia and brain endothelial cells expressed all of the recognized HCV entry receptors. Two independently derived brain endothelial cell lines, hCMEC/D3 and HBMEC, supported HCV entry and replication. These processes were inhibited by antibodies against the entry factors CD81, scavenger receptor BI, and claudin-1; by interferon; and by reagents that inhibit NS3 protease and NS5B polymerase. HCV infection promotes endothelial permeability and cellular apoptosis. **CONCLUSIONS: Human brain endothelial cells express functional receptors that support HCV entry and replication. Virus infection of the CNS might lead to HCV-associated neuropathologies.**

Keywords: Virus Tropism; HCVpp; HCVcc; Neurologic Defect.

Hepatitis C virus (HCV) is an enveloped positive-strand RNA virus classified in the *Hepacivirus* genus of the Flaviviridae family. Worldwide, approximately 170 million individuals are infected with HCV that leads to a progressive liver disease. Infection is associated with a variety of extrahepatic syndromes, including cryoglobulinemia, glomerulonephritis, and central nervous system (CNS) abnormalities.¹

Although HCV is primarily a hepatotropic virus, genomic viral RNA has been detected in peripheral blood mononuclear cells, cerebrospinal fluid, and the brain of chronically infected patients with neuropathologic abnormalities (reviewed in Morgello² and Weissenborn et al³). At present, there is no small animal model to study HCV pathobiology and studies on tropism are limited to humans. Analysis of HCV sequences derived from peripheral blood mononuclear cells, brain, and liver show tissue-specific differences, suggesting independent evolution at different anatomic sites.⁴⁻⁶

Virus tropism is likely to be defined at multiple stages of the viral life cycle, including entry, replication, and assembly. The availability of retroviral pseudoparticles bearing HCV glycoproteins (HCVpp) and the recently reported JFH-1 strain of HCV that replicates and assembles infectious particles in cell culture (HCVcc) have enabled considerable advances in our understanding of the receptors involved in HCV internalization.^{7,8} Recent evidence shows a number of host cell molecules to be important for HCV entry: low-density lipoprotein receptor (LDL-R), tetraspanin CD81, scavenger receptor class B member I (SR-BI), and the tight junction proteins claudin-1 and occludin.⁷

To date, the majority of reports have studied HCV replication in hepatocytes or hepatoma-derived cells. However, HCV has been reported to replicate to low levels in nonhepatic cells,^{9,10} suggesting that additional cellular reservoirs exist. In this study, we show that human brain microvascular endothelium, the major component of the blood-brain barrier (BBB), expresses all major HCV entry receptors. Furthermore, 2 independently derived brain

Abbreviations used in this paper: apoE, apolipoprotein E; BBB, blood-brain barrier; CNS, central nervous system; HCVcc, cell culture-derived hepatitis C virus; HCVpp, hepatitis C virus pseudotype particles; HIV, human immunodeficiency virus; LDL-R, low-density lipoprotein receptor; qRT-PCR, quantitative reverse-transcription polymerase chain reaction; SR-BI, scavenger receptor BI; TUNEL, terminal deoxynucleotidyl transferase-mediated deoxyuridine triphosphate nick-end labelling; VSV-Gpp, vesicular stomatitis virus G pseudoparticles.

© 2012 by the AGA Institute

0016-5085/\$36.00

doi:10.1053/j.gastro.2011.11.028

microvascular endothelial cell lines support HCV entry and replication,^{11,12} providing a potential mechanism for HCV to infect the CNS.

Materials and Methods

Cells, Reagents, and Clinical Material

Huh-7 and 293T cells were provided by C. Rice (Rockefeller University, New York, NY) and U87 cells by American Type Culture Collection (Manassas, VA). All cells were maintained in Dulbecco's modified Eagle medium supplemented with 10% fetal bovine serum, 1% nonessential amino acids/1% penicillin/streptomycin (Invitrogen). hCMEC/D3 cells were maintained in complete EGM-2 medium (Lonza, United Kingdom).¹² HBMEC cells were maintained in RPMI supplemented with 10% fetal bovine serum/10% NuSerum and 30 $\mu\text{g}/\text{mL}$ Endothelial Cell Growth Supplement (BD Biosciences) as well as 1% nonessential amino acids/1% penicillin/streptomycin (Invitrogen). Human umbilical vein endothelial cells and liver sinusoidal endothelial cells were isolated as previously described.¹³ Clinical material is further described in Supplementary Materials and Methods.

The primary antibodies were anti-NS5A 9E10 (C. Rice, Rockefeller University), anti-CD81 (2.131),¹⁴ anti-SR-BI (V. Flores, Pfizer), anti-claudin-1 (Abnova and R&D), anti-claudin-1 polyclonal sera,¹⁵ anti-occludin (Invitrogen), anti-ZO-1 (Invitrogen), anti-LDL-R (Progen), anti-apolipoprotein E (mAb23),¹⁶ anti-von Willebrand factor (Dako), anti-glial fibrillary acidic protein (Dako), anti-CD63 (Dako), anti-CD163 (Novocastra), and anti-E2 (9/27, 11/27, and 3/11).¹⁷ Immunoglobulin (Ig) from healthy volunteers and chronically HCV-infected donors was purified by protein G affinity chromatography. Fluorescent secondary antibodies Alexa Fluor 488 and 594 anti-mouse, anti-human, anti-rat, and anti-rabbit IgG were obtained from Invitrogen.

Flow Cytometric Analysis of Receptor Expression

For CD81, SR-BI, claudin-1, ZO-1, and LDL-R staining, cells were incubated with monoclonal antibodies at 2 $\mu\text{g}/\text{mL}$ in phosphate-buffered saline containing 1% bovine serum albumin/0.01% sodium azide for 20 minutes at 37°C. For occludin staining, cells were fixed with 1% paraformaldehyde and permeabilized with phosphate-buffered saline/1% bovine serum albumin/1% saponin. Bound antibodies were detected with Alexa 488 secondary antibodies and quantified by flow cytometry using a FACSCalibur (BD Biosciences) and FlowJo software (TreeStar, Ashland, OR).

Laser Scanning Confocal Microscopy

Sequential 5- μm sections of formalin-fixed, paraffin-embedded normal brain tissue from 5 subjects were dewaxed and rehydrated and microwave antigen retrieval was performed in EDTA buffer. Cell lines were plated on collagen-coated coverslips (Fisher Scientific, United Kingdom) and 24 hours later fixed with ice-cold methanol (claudin-1, occludin, ZO-1, LDL-R) or 3% paraformaldehyde (CD81). After incubation with primary antibodies (2 $\mu\text{g}/\text{mL}$), cells were incubated with Alexa 488 secondary antibodies, counterstained with 4',6-diamidino-2-phenylindole, and viewed by laser scanning confocal microscopy on a Zeiss MetaHead microscope with a 100 \times oil immersion objective.

HCVpp and HCVcc Genesis and Infection

Luciferase reporter pseudoparticles expressing a panel of HCV envelope glycoproteins (HCVpp), vesicular stomatitis virus G glycoprotein (VSV-Gpp), or a no-envelope control were generated as previously reported.¹⁷ Virus-containing medium was added to cells in 96-well plates seeded at 7.5×10^3 cells/cm² and incubated for 72 hours. Cells were lysed, and luciferase activity was measured (Lumat LB9507 luminometer). Infectivity is expressed as relative light units, where the no-envelope signal is subtracted from HCVpp or VSV-Gpp signals.

Plasmids encoding chimeric SA13/JFH¹⁸ or J6/JFH¹⁹ were used to generate RNA as previously described.¹⁹ Briefly, RNA was electroporated into Huh-7.5 cells, and supernatants were collected at 72 and 96 hours and stored at -80°C. Infected cells were fixed with ice-cold methanol and stained for NS5A with monoclonal antibody 9E10 and isotype-matched Alexa 488-conjugated anti-mouse IgG2a. NS5A-positive foci were enumerated, and infectivity was expressed as focus-forming units per milliliter.

Neutralization of HCV Infection

Cells were seeded in 96-well plates at 7.5×10^3 cells/cm². After 24 hours, cells were incubated with anti-receptor or irrelevant IgG control monoclonal antibodies at 10 $\mu\text{g}/\text{mL}$ for 1 hour, and HCVcc or HCVpp was added and incubated for 72 hours. Anti-E2 monoclonal antibodies or HCV-positive IgG were incubated with virus for 1 hour before infecting target cells. Alternatively, cells were incubated with virus for 8 hours, unbound virus was removed by washing, and cells were incubated with neutralizing antibodies. For HCVpp, cells were lysed and luciferase activity was measured. For HCVcc, cells were fixed with ice-cold methanol and stained for NS5A. The percent neutralization was calculated relative to the irrelevant IgG.

Real-Time Reverse-Transcription Polymerase Chain Reaction

Purified cellular or tissue RNA samples were amplified for HCV RNA (Primer Design Ltd) in a quantitative reverse-transcription polymerase chain reaction (qRT-PCR) as per the manufacturer's guidelines (CellsDirect Kit; Invitrogen) and fluorescence was monitored in an MxPro-3000 PCR machine (Stratagene). Comparison of a panel of housekeeping genes in brain and liver RNA confirmed GAPDH as a stably expressed reference gene. Hence, GAPDH was included as an endogenous control for amplification efficiency and RNA quantification. The assay cutoff was 100 copies.

Permeability and Apoptosis Assays

hCMEC/D3 cells were seeded on collagen I-coated Transwell filters (0.4 μm ; pore size, 1.1 cm²; Sigma-Aldrich) and cultured as described.²⁰ Cells were infected with HCVcc, with or without prior incubation with anti-HCV IgG for 48 hours, or a combination of tumor necrosis factor α and interferon gamma for 24 hours before measuring paracellular permeability by using the clearance method.²¹ hCMEC/D3 and Huh-7 cells were seeded on collagen-coated coverslips and infected with J6/JFH or SA13/JFH. After 72 hours, cells were fixed and terminal deoxynucleotidyl transferase-mediated deoxyuridine triphosphate nick-end labeling (TUNEL) staining was performed as per the manufacturer's instructions (Invitrogen).

Statistical Analysis

Statistical analyses were performed using Student *t* test in Prism 4.0 (GraphPad, La Jolla, CA), with *P* < .05 considered significant.

Results

HCV RNA Load in Brain and Liver Tissue

To quantify HCV RNA levels in the brain and liver of infected subjects, cellular RNA was extracted from human brain (cerebellum, medulla, white and grey matter) and liver from 10 HCV-infected and 3 uninfected subjects as previously described.²² HCV RNA was amplified from the liver sample of all infected subjects tested but not from HCV-seronegative individuals. HCV RNA was detected in brain tissue from 4 of 10 HCV-infected individuals, independent of human immunodeficiency virus (HIV) status (Table 1). In those individuals in whom HCV was detectable in the brain, viral RNA quantities were 1000 to 10,000 times lower than in the matched liver samples (Table 1).

Human Brain Endothelium Express HCV Receptors

To investigate the expression of HCV receptors in the brain, sequential sections from normal and HCV-infected brain samples were stained with antibodies specific for HCV receptors and cell lineage markers: von Willebrand factor (endothelium), glial fibrillary acidic protein, CD68 (macrophages/microglia), and CD163 (perivascular macrophages). Microvascular endothelium costained with endothelial-specific von Willebrand factor and HCV receptors CD81, SR-BI, claudin-1, occludin, and LDL-R (Figure 1 and Supplementary Figure 1). Comparable patterns of viral receptor staining were observed independent of HCV status. CD81, claudin-1, and occludin were also expressed on neurons and CD81 on astrocytes. In con-

trast, SR-BI expression was restricted to microvascular endothelium (Supplementary Figure 1).

Human Brain Endothelial Cells Support HCV Entry and Replication

Two independently derived brain microvascular endothelial cell lines, hCMEC/D3 and HBMEC,^{11,12} express all the HCV entry factors (Figure 2A-C). In contrast, human umbilical vein endothelial cells and liver sinusoidal endothelial cells express low levels of SR-BI and undetectable claudin-1 (Figure 2C), suggesting that expression of the full complement of HCV receptors is specific to brain endothelial cells. Costaining of brain endothelial cells with antibodies specific for CD81, SR-BI, and claudin-1 confirmed expression of all receptors (Supplementary Figure 2).

To ascertain whether viral receptors on brain endothelial cells are functionally active, we studied the ability of HCVpp to infect brain endothelial cells. HCVpp infected hCMEC/D3, HBMEC, primary hepatocytes, and control Huh-7 hepatoma cells, whereas there was no detectable luciferase signal in human umbilical vein endothelial cells and liver sinusoidal endothelial cells (Figure 3A). VSV-Gpp infected all cells with different efficiencies, most likely reflecting cell type-dependent differences in reporter expression. Normalizing HCV infection relative to VSV-G shows comparable HCV entry rates in brain endothelial cells and primary hepatocytes (Figure 3B). Furthermore, HCVpp expressing diverse envelope glycoproteins cloned from several acutely infected subjects infected hCMEC/D3 cells (Figure 3C). HCVpp infection of hCMEC/D3 or HBMEC was inhibited by anti-HCV E2 and patient-derived pooled Ig, confirming glycoprotein-dependent entry (Figure 3D). To investigate the receptor dependency of HCVpp infection of brain endothelial cells, we assessed the ability of monoclonal antibodies specific for

Table 1. HCV RNA Viral Loads in Human Brain Tissue

Sample ID	Age (y)	Sex	HIV status	HCV status	Liver pathology	Cause of death	Postmortem interval (h)	HCV RNA load (10 mg tissue)				
								Liver	Cerebral grey matter	Cerebral white matter	Cerebellum	Medulla
10034	49	Male	Positive	Positive	Cirrhosis	Pneumonia	4.5	6.1×10^8	3.8×10^4	5.4×10^3	4.7×10^3	6.4×10^3
10066	54	Female	Positive	Positive	Cirrhosis	Probable sepsis	7	1.8×10^8	—	1.7×10^2	—	—
20024	62	Male	Positive	Positive	Fibrosis	Bronchiolitis, emphysema, aortic stenosis	4	9.4×10^8	1.1×10^5	—	—	—
40007	53	Male	Negative	Positive	Cirrhosis	End-stage liver disease	11.5	9.0×10^6	4.0×10^2	8.5×10^2	—	—
10016	58	Female	Positive	Positive	Cirrhosis	Extensive metastatic calcifications and congestive heart failure	17	4.2×10^8	—	—	—	—
10027	39	Male	Positive	Positive	Cirrhosis	Severe cachexia, HIV encephalitis	4	1.4×10^9	—	—	—	—
10086	48	Female	Positive	Positive	Cirrhosis	Pneumonia and sepsis	7.5	1.1×10^9	—	—	—	—
20028	49	Male	Positive	Positive	Cirrhosis	Cardiac and liver failure	6	4.7×10^8	—	—	—	—
40003	54	Male	Negative	Positive	Cirrhosis	Sepsis, pneumonitis, end-stage liver disease, and renal failure	14.5	3.1×10^8	—	—	ND	ND
537	44	Male	Negative	Positive	Minimal steatosis, fibrosis, and inflammation	Pneumonia (<i>Pneumocystis carinii</i> , cytomegalovirus)	27	1.9×10^9	—	—	ND	ND

NOTE. HCV RNA from matched brain and liver tissue from HCV-positive clinical samples was quantified by qRT-PCR and normalized to GAPDH. Virus was detected in the liver of all 10 subjects and in the brain tissue of 4 subjects. Viral load was approximately 1000-fold lower in the brain compared with the liver. HCV E1 sequence variation between liver and plasma was previously reported for samples 10034, 20024, 20028, and 40007.²⁹ ND, not determined.

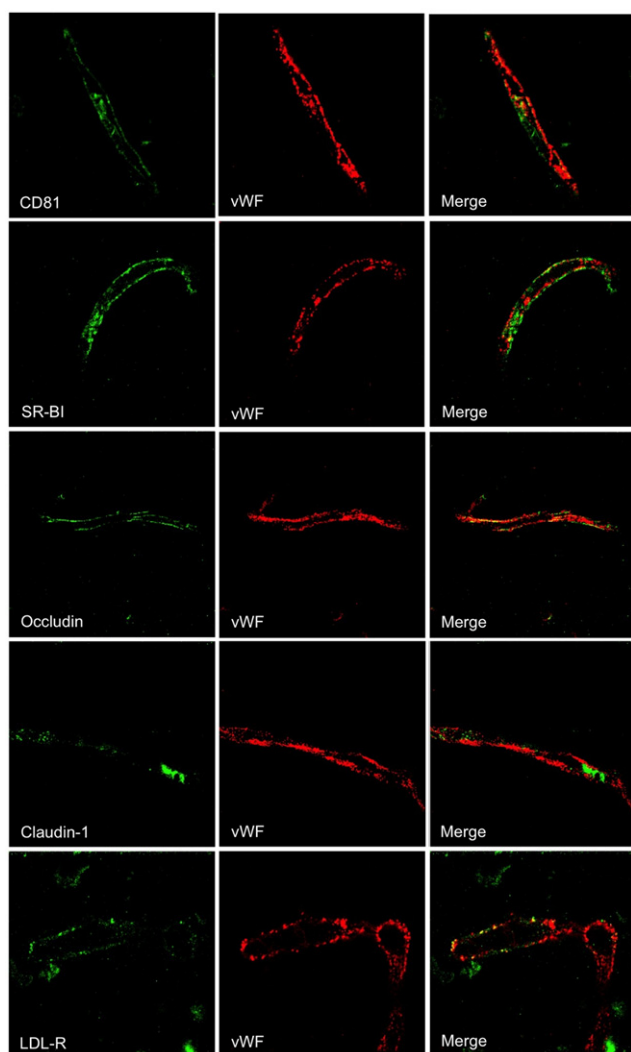


Figure 1. HCV receptor expression in human brain tissue. Formalin-fixed, paraffin-embedded brain sequential sections were costained with antibodies specific for von Willebrand factor (vWF), a marker for endothelial cells, and HCV receptors SR-BI, CD81, claudin-1, occludin, and LDL-R. Brain endothelium expressed all the factors required for HCV entry. Original magnification 100 \times .

viral receptors to neutralize infection. Antibodies specific for CD81, SR-BI, and claudin-1 significantly reduced HCVpp infection of hCMEC/D3 and HBMEC (Figure 3D) but had no effect on VSV-Gpp infection (Supplementary Figure 3), showing a common receptor-dependent pathway of entry in these cell lineages.

Given the permissive nature of brain microvascular endothelial cells for HCV glycoprotein-dependent pseudoparticle infection, we investigated their ability to support replication of 2 chimeric HCVcc JFH-1 viruses expressing genotype 2a strain J6¹⁹ or genotype 5a strain SA13 structural proteins.¹⁸ As controls, we included permissive Huh-7 and nonpermissive U87 cell lines.¹⁰ Cells were incubated with increasing concentrations of virus, fixed and infection visualized by staining for viral non-structural protein NS5A. Both HCV strains infected hCMEC/D3 cells with an approximate 100- to 300-fold re-

duced titer compared with Huh-7 cells (Figure 4A). HCVcc showed a 100-fold reduced titer in HBMEC compared with hCMEC/D3 cells. Interferon alfa inhibited HCVcc infection of all cell lines (Figure 4A). Unsurprisingly, we failed to detect NS5A in U87 cells (data not shown). To confirm de novo HCV replication and ascertain the sensitivity of endothelial cells to antiviral agents, we compared the ability of several protease and polymerase inhibitors to inhibit HCV replication in hCMEC/D3 and Huh-7 cells. All antiviral agents significantly reduced HCV infection of both cell types (Figure 4B), with the majority of agents showing greater efficacy in hCMEC/D3 cells.

Pretreatment of hCMEC/D3 and Huh-7 cells with antibodies specific for CD81, SR-BI, or claudin-1 significantly reduced HCVcc infection (Figure 4C), confirming our earlier observations with HCVpp. Infectious HCVcc particle assembly is dependent on the lipoprotein synthesis machinery of the host cell leading to the genesis of lipoviral particles.²³ Several reports have shown a key role for apolipoprotein E (ApoE) in HCV assembly and entry.^{8,24} Because ApoE is known to bind SR-BI and several members of the LDL-R family, we investigated the effect(s) of antibodies targeting ApoE and LDL-R on HCV infection of hCMEC/D3. Anti-ApoE and anti-LDL-R significantly reduced infection of hCMEC/D3 while showing a more modest effect on Huh-7 cells (Figure 4C).

To investigate whether HCV initiates a spreading infection in hCMEC/D3, virus was allowed to enter and infect endothelial or Huh-7 cells for 8 hours, unbound virus was removed by extensive washing, and receptor-specific neutralizing antibodies were added. Virus-infected cells were incubated for 72 hours to allow secondary transmission events to occur and the number of NS5A-expressing infected cells enumerated. Infected foci of NS5A-expressing hCMEC/D3 cells were readily observable, indicating viral spread (Figure 4C). Although receptor-specific antibodies reduced primary infection of hCMEC/D3 cells, antibodies specific for CD81 or ApoE significantly reduced secondary infection, showing a role for cellular CD81 and virus-associated ApoE in viral dissemination between brain endothelial cells (Figure 4D). This ApoE dependency in the endothelial cultures is consistent with endogenous ApoE expression in hCMEC/D3 cells (data not shown).

To confirm a productive infection of brain endothelial cells, HCV SA13/JFH-infected hCMEC/D3 or Huh-7 cells were sequentially harvested to quantify the frequency of NS5A-expressing cells and HCV RNA levels over time. HCV RNA was first detected in hCMEC/D3 cells at 24 hours and levels increased significantly by 48 hours, in parallel with the increasing number of NS5A-expressing cells (Figure 5). There was no detectable viral RNA at 12 hours after infection, showing de novo rounds of viral replication. HCV RNA and NS5A expression in Huh-7 cells increased over time (Figure 5). At 48 hours, the level of HCV RNA in Huh-7 cells was approximately 1000-fold higher than in hCMEC/D3 cells (Figure 5A). However, normalizing HCV RNA to the number of NS5A-positive cells in each culture at 48 hours showed 133 and 1067

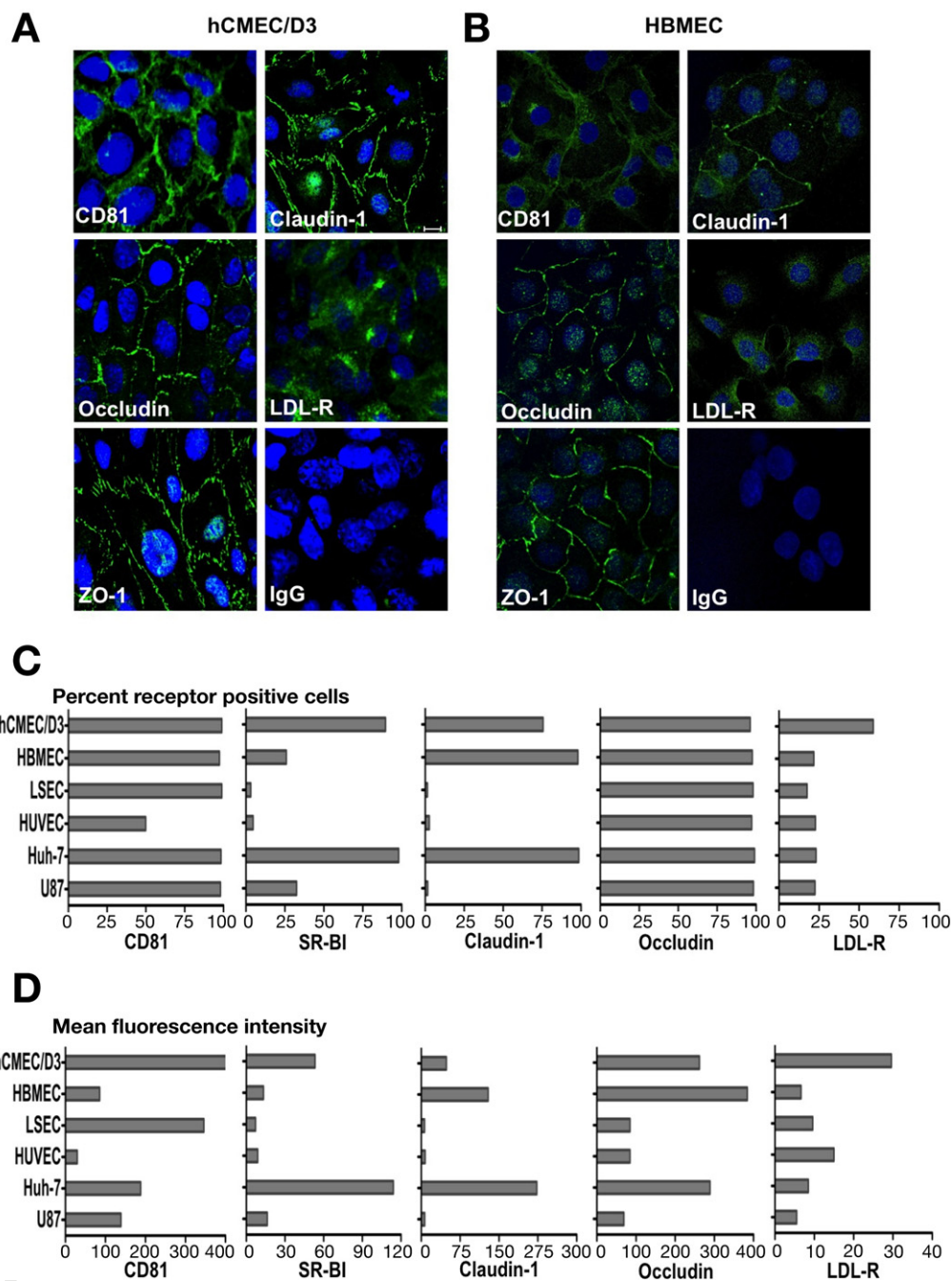


Figure 2. HCV receptor expression in microvascular endothelial cells. CD81, claudin-1, occludin, ZO-1, and LDL-R expression in (A) hCMEC/D3 or (B) HBMEC. Flow cytometric analysis of HCV entry factor expression in hCMEC/D3, HBMEC, liver sinusoidal endothelial cells (LSEC), and human umbilical vein endothelial cells (HUVEC), together with the permissive Huh-7 hepatoma and nonpermissive U87 cells. (C and D) The percent receptor-positive cells and mean fluorescent intensity (MFI) are shown. Anti-receptor antibodies showed negligible binding to receptor-negative Chinese hamster ovary cells with MFI values between 4 and 8. Isotype control antibodies gave MFI values between 5 and 11 for all cells tested. Data are representative of 2 independent experiments.

copies/infected cell for hCMEC/D3 and Huh-7 cells, respectively, reflecting only a ~10-fold difference in viral genomic burden for the 2 cell types.

miR-122 is a liver-specific microRNA that is required for efficient HCV replication and is considered a therapeutic target for antiviral intervention.²⁵ qRT-PCR confirmed that miR-122 was not detectable in human brain tissue, whereas abundant levels were observed in all liver samples studied. We failed to detect miR-122 expression in hCMEC/D3 cells by qRT-PCR or Northern blot (Supplementary Figure 4A-C). Importantly, transfection of hCMEC/D3 to express functionally active miR-122 RNA duplexes²⁵ failed to promote HCV infection (Supplementary Figure 4D-F), showing that

HCV replication in hCMEC/D3 cells is miR-122 independent.

Brain Endothelial Cells Release Infectious Virus

To ascertain whether brain endothelial cells can release virus that is infectious for hepatocytes, hCMEC/D3, Huh-7, or nonpermissive U87 cells were infected with HCVcc SA13/JFH for 12 hours at a comparable multiplicity of infection and unbound virus was removed by washing. Virus-infected cells were incubated at 37°C for 72 hours, extracellular medium was collected, and cells were fixed and stained for NS5A. Levels of infectious virus in the medium

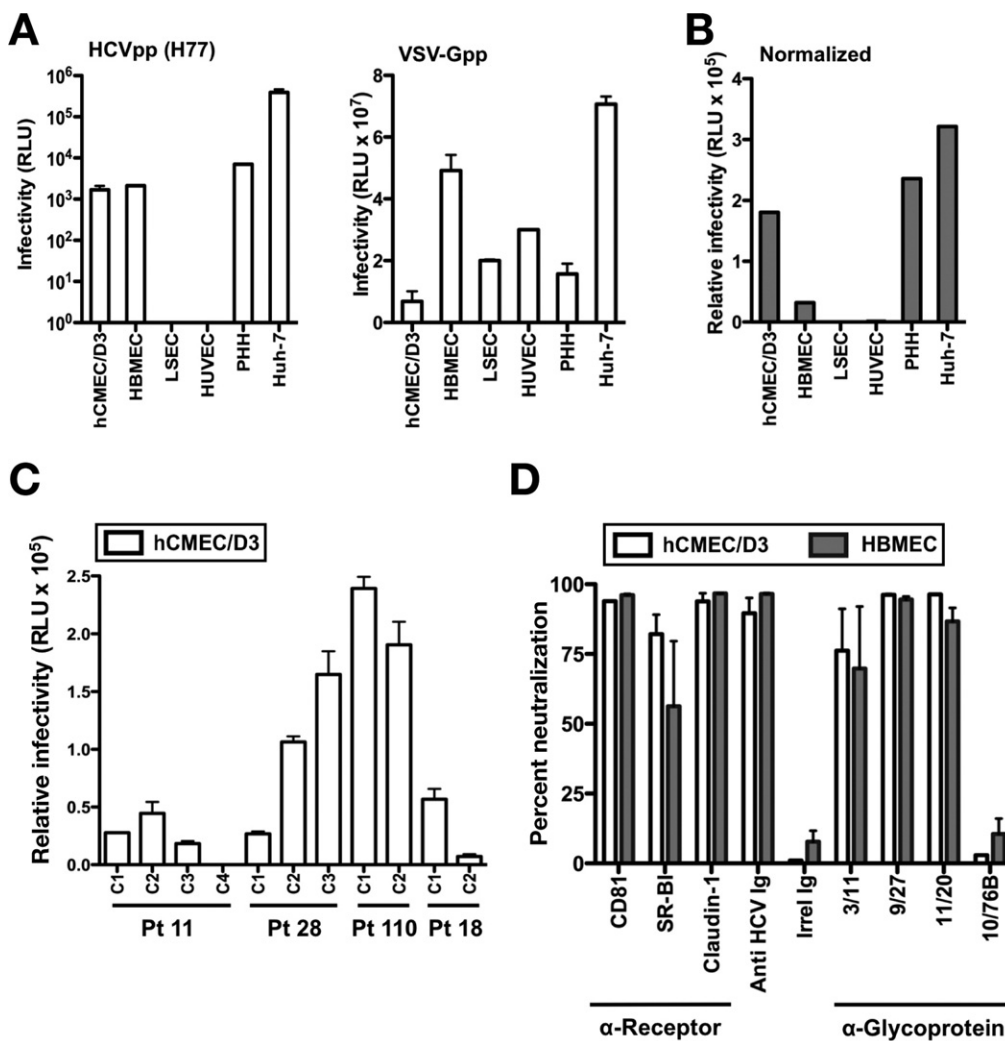


Figure 3. Microvascular brain endothelial cells support HCV entry. HCVpp-H77 infection of hCMEC/D3, HBMEC, human umbilical vein endothelial cells (HUVEC), liver sinusoidal endothelial cells (LSEC), primary human hepatocytes (PHH), and Huh-7 cells. (A) HCVpp and VSV-Gpp entry is expressed as relative light units (RLU). (B) Normalized HCVpp entry relative to VSV-Gpp. (C) Infectivity of HCVpp bearing primary envelopes cloned from 4 acutely infected patients (Pt 11, Pt 28, Pt 110, and Pt 18) for hCMEC/D3. HCVpp infection of hCMEC/D3 and HBMEC was neutralized by antibodies targeting CD81, SR-BI, or claudin-1 and viral glycoproteins (anti-HCV E2 3/11, 9/27, 11/20, and pooled anti-HCV IgG). (D) Anti-HIV 10/76B and irrelevant globulin had no effect. Data are representative of 3 independent experiments.

were determined by inoculating naïve Huh-7.5 cells. Similar numbers of HCV-infected hCMEC/D3 and Huh-7 cells were observed; however, the level of infectious virus released from hCMEC/D3 cells over an 8-hour period was 68 focus-forming units, compared with 1680 focus-forming units released from Huh-7 cells (Supplementary Figure 5). We attempted to inoculate naïve hCMEC/D3 cells with viral supernatant from HCVcc-infected hCMEC/D3 cells and failed to detect infection, most likely because of the low levels of virus released from infected hCMEC/D3 cultures (data not shown). To ascertain whether the low levels of infectious virus in the hCMEC/D3 culture medium could be attributed to a persisting viral inoculum, we titered the extracellular media collected from virus-inoculated U87 cells and failed to detect infectious virus. Furthermore, medium collected 12 hours after virus inoculation contained no detectable infectious virus. In summary, these data show that brain endothelial cells release low levels of HCV that are infectious for hepatoma cells.

HCV Increases Endothelial Cell Permeability

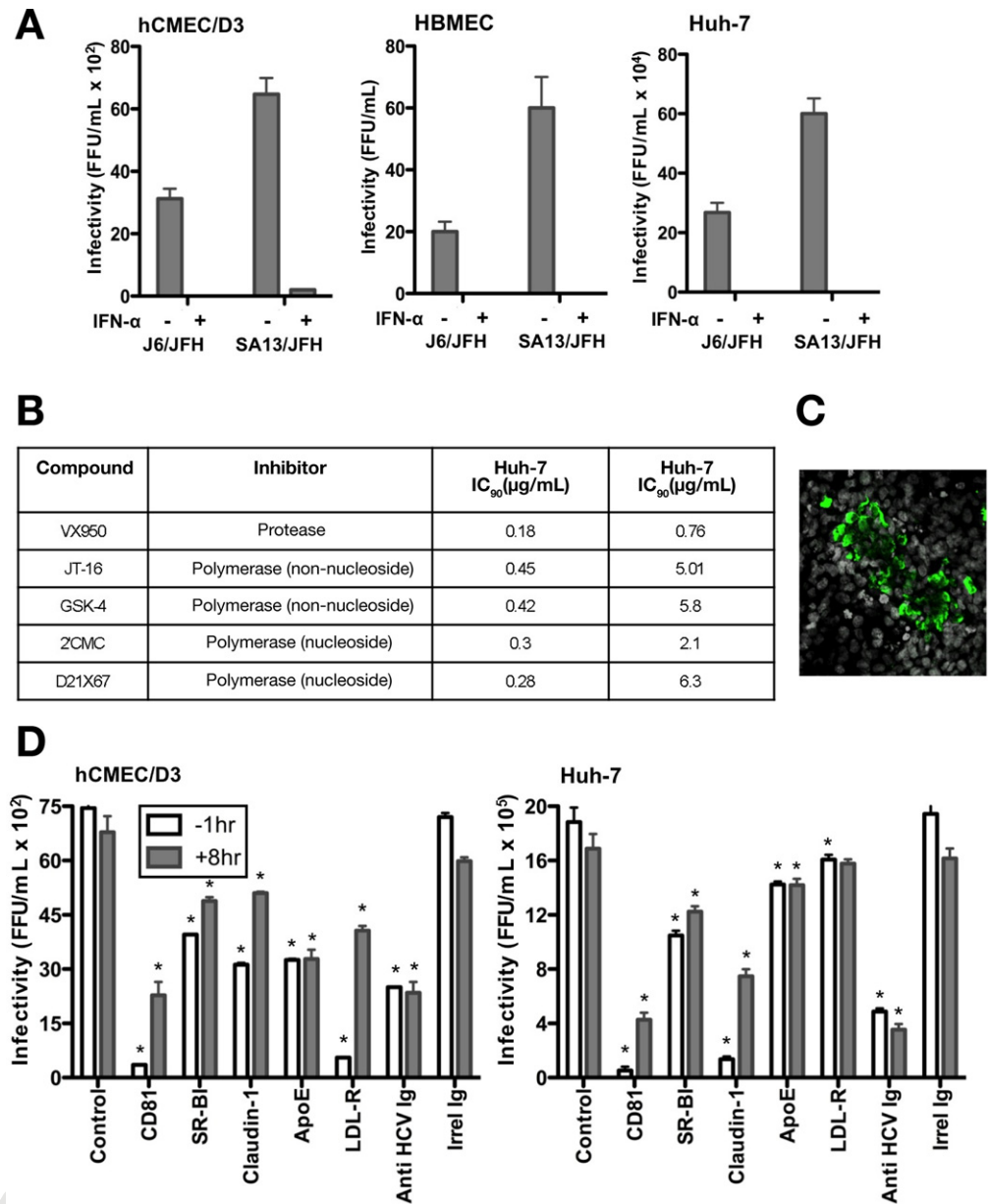
To investigate whether HCV infection affects hCMEC/D3 paracellular permeability, confluent cells were

allowed to polarize and 70-kilodalton fluorescein isothiocyanate/dextran flux was measured. Human tumor necrosis factor α /interferon gamma treatment or HCV infection significantly increased hCMEC/D3 paracellular permeability (Figure 6A), showing that HCV can disrupt endothelial cell integrity. Neutralization of HCV infection with pooled anti-HCV patient Ig restored hCMEC/D3 impermeability, showing a direct effect of infection (Figure 6A). We noted that HCV-infected hCMEC/D3 cells showed evidence of cytopathicity in association with NS5A expression. To ascertain whether HCV induced apoptosis, we stained infected hCMEC/D3 and Huh-7 cells for DNA strand breaks using TUNEL. A low frequency of HCV-infected Huh-7 cells stained positive for both TUNEL and NS5A.²⁶ In contrast, all the NS5A-positive endothelial cells were TUNEL positive, showing a direct effect of infection on brain endothelial cell apoptosis (Figure 6B).

Discussion

HCV infection leads to progressive liver disease, which has been associated with extrahepatic syndromes, including CNS abnormalities.³ There is a growing body of

Figure 4. Microvascular brain endothelial cells support HCV replication. hCMEC/D3, HBMEC, and Huh-7 cells were infected with HCVcc J6/JFH or SA13/JFH, and infection was expressed as focus forming units per milliliter (FFU/mL). (A) Interferon alfa (IFN- α ; 100 IU/mL) inhibited infection of all cell lines. hCMEC/D3 and Huh-7 cells were infected with HCVcc J6/JFH for 8 hours and treated with increasing concentrations of antiviral drugs targeting HCV protease and polymerase. (B) The concentration of inhibitor that reduced infection by 90% was determined (IC_{90}). (C) Focus of HCV NS5A-expressing hCMEC/D3 cells. (D) Antibodies specific for HCV entry factors CD81, SR-BI, claudin-1, LDL-R, and ApoE, anti-HCV Ig, or irrelevant Ig were incubated with hCMEC/D3 and Huh-7 cells for 1 hour before (white bars) or 8 hours after (black bars) infection. Infected cells were incubated for 72 hours and NS5A-positive cells enumerated. Statistically significant neutralization relative to the irrelevant IgG is indicated (* $P < .0001$). Data are representative of 3 independent experiments.



literature on mild neurocognitive impairment in chronic HCV infection that is independent of hepatic encephalopathy.²⁷ However, there is a lack of studies to investigate whether cells of the CNS support HCV replication. In this study, we report that all of the essential HCV receptors are expressed on brain microvascular endothelial cells. Indeed, the microvascular endothelia were the only cell type in the brain that expressed all the factors required for HCV entry. To our knowledge, this is the first study to investigate the expression of HCV receptors in the human brain. Microvascular endothelial cells are a major component of the BBB²⁸ and may provide a portal for HCV to infect the CNS.

Quantification of HCV RNA from matched samples of white and grey matter, cerebellum, medulla, liver, and plasma revealed that, in clinical samples with detectable brain HCV, the viral load was 1000- to 10,000-fold

lower in brain compared with liver from the same subject. HCV RNA was detected in at least one brain region from 4 of 10 HCV-infected subjects, independent of HIV coinfection status. Although quantities of viral RNA from the brain and liver varied widely between clinical samples, in general a lower viral load was associated with a higher postmortem interval, suggesting RNA degradation in some samples over time. Variation between brain-, plasma-, and liver-derived HCV E1 and 5' untranslated region sequences has previously been reported in this cohort, supporting the hypothesis that HCV replicates and evolves within the brain.²⁹ However, care is needed when interpreting the physiologic relevance of detecting HCV RNA genomes. It is worth noting that 6 HCV-infected subjects had no detectable viral RNA in the brain, despite having comparable levels of viral RNA in the liver and plasma

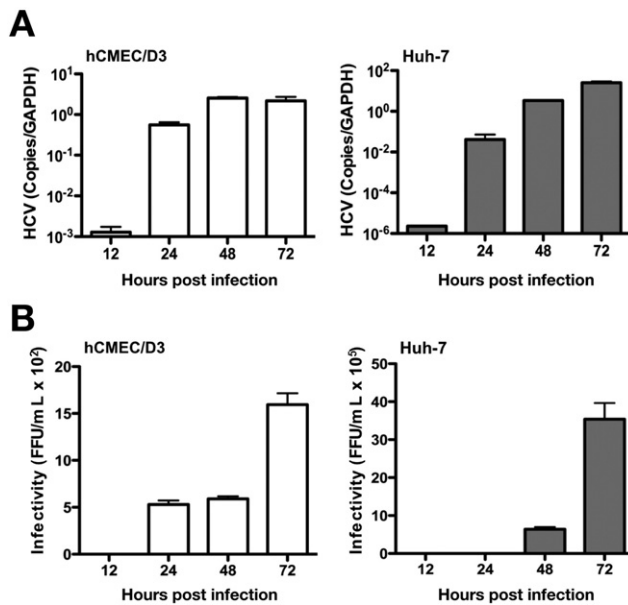


Figure 5. HCV RNA and antigen expression in brain endothelial and hepatoma cells. hCMEC/D3 and Huh-7 cells were infected with HCVcc SA13/JFH for 12 hours, and unbound virus was removed by washing. (A) HCV RNA copies and (B) the frequency of NS5A-positive cells were determined at the indicated times. Infectivity is presented as focus forming units per milliliter (FFU/mL) and HCV RNA copies relative to GAPDH.

(Supplementary Materials and Methods) to 4 subjects with no detectable HCV RNA in the brain.

There have been significant difficulties in visualizing HCV antigen-expressing hepatocytes in the liver that most likely reflect the low viral burden at a cellular level.^{30,31} Our quantification of HCV RNA in brain tissue compared with liver suggests that detecting HCV antigen in the brain will be technically challenging, and current imaging methodologies lack the sensitivity to reliably detect HCV-infected cells in the CNS. Indeed, our attempts to show NS3 or NS5A HCV antigen in brain or liver samples from subjects in this study have failed to provide robust signals (data not shown). Previous studies have reported the presence of HCV RNA in microglia and astrocytes isolated using laser capture microdissection.^{32,33} However, our experiments show that astrocytes and microglia lack expression of several receptors required for HCV entry.¹⁰

Our studies show that 2 independently derived brain microvascular endothelial cell lines, hCMEC/D3 and HBMEC, support HCVpp entry. Infection was inhibited by antibodies specific for CD81, SR-BI, claudin-1, or E2 glycoprotein, showing a common receptor-dependent entry pathway to that reported for hepatocytes and hepatoma-derived cell lines.^{34,35} These observations, along with our recent report that neuroepithelioma cell lines derived from peripheral tumors support efficient HCVpp infection,¹⁰ show that viral entry is not restricted to hepatocytes. Importantly, messenger RNA and protein profiling databases show that CD81, SR-BI, claudin-1, and occludin are expressed in epithelial and endothelial cells from various tissues,^{36,37} raising the possibility that other cell types may support HCV infection. Our data support the pres-

ence of functional entry receptors in BBB endothelial cells but not endothelial cells derived from umbilical vein and liver sinusoids.

Given the permissivity of brain endothelial cells for HCVpp entry, we investigated their ability to support HCVcc replication. HCV-infected hCMEC/D3 cells release low levels of virus that can infect hepatoma cells and showed evidence for a spreading infection that is CD81 dependent. Recent reports highlighting the role of ApoE in HCV assembly^{8,24} and the targeting of ApoE-containing nanoparticles across the BBB^{38,39} prompted us to investigate a role for ApoE in brain endothelial cell infection. Interestingly, antibodies targeting ApoE effectively neutralized HCV infection of hCMEC/D3 cells, despite mod-

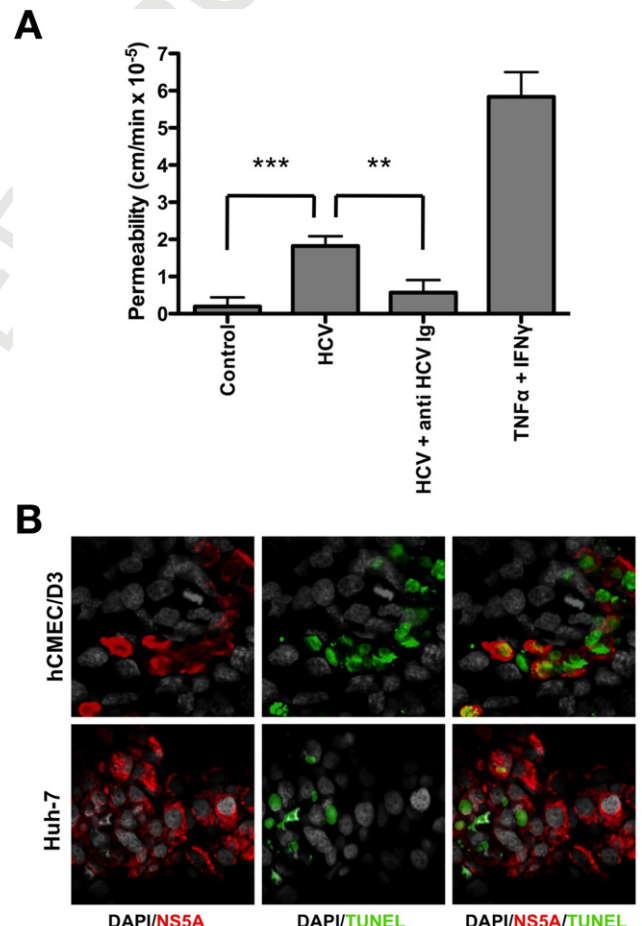


Figure 6. HCV increases brain endothelial permeability and apoptosis. hCMEC/D3 cells were cultured on permeable filters and infected with HCVcc SA13/JFH for 72 hours or treated with recombinant human tumor necrosis factor α and interferon gamma at 10 ng/mL for 24 hours. Paracellular permeability to fluorescein isothiocyanate/dextran 70 kilodaltons was measured. (A) HCV induced a significant increase in permeability ($P < .001$), which was inhibited by anti-HCV Ig ($P < .05$). Significant increases in permeability were also observed in response to tumor necrosis factor α /interferon gamma (IFN- γ). (B) hCMEC/D3 and Huh-7 cells were infected with HCVcc SA13/JFH for 72 hours at comparable multiplicities of infection and costained for NS5A (red) and DNA strand breaks by using TUNEL (green). Although some apoptosis was associated with HCV-infected Huh-7 cells, apoptosis was pronounced in infected hCMEC/D3 cells. Data are representative of 3 independent experiments.

406
407
408
409
410
411
412
413
414
415
416
417
418
419
420
421
422
423
424
425
426
427
428
429
430
431
432
433
434
435
436
437
438
439
440
441
442
443
444
445
446
447
448
449
450
451
452
453
454
455
456
457
458
459
460
461
462
463

406
407
408
409
410
411
412
413
414
415
416
417
418
419
420
421
422
423
424
425
426
427
428
429
430
431
432
433
434
435
436
437
438
439
440
441
442
443
444
445
446
447
448
449
450
451
452
453
454
455
456
457
458
459
460
461
462
463

BASIC AND
TRANSITIONAL
TACREAS

ROF06

AQ: 16

est neutralization of Huh-7 cells, suggesting a greater role for ApoE in virus infection of brain endothelial cells.

The BBB limits the passage of substances from blood to the CNS by the presence of tight junctions between endothelial cells and by receptor-mediated efflux transport systems that restrict the entry of hydrophilic molecules to the brain.²⁸ Multidrug resistance proteins, including P-glycoprotein, restrict the transport of many drugs across the BBB, including antivirals that may contribute to the development of “sanctuary sites,” allowing pathogens (eg, HIV-1) to replicate in the brain of drug-treated patients.⁴⁰ In the present study, HCV replication was inhibited by antiviral agents targeting NS3 protease and NS5B polymerase enzymes *in vitro*.

Disruption of BBB integrity can lead to an infiltration of pathogens, cytokines, and immune cells to the brain parenchyma as reported for HIV-1 and West Nile viruses.^{41,42} hCMEC/D3 infection led to increased HCV RNA and antigen expression over time, with a cytopathic effect that associated with TUNEL staining and increased permeability to the paracellular permeability marker FD-70. These data support a model in which HCV infection may compromise BBB integrity, with implications for brain homeostasis in HCV infection.

In conclusion, we show that brain microvascular endothelium expresses all the major viral receptors required for HCV infection. Two brain endothelial cell lines support HCV entry and replication, in which infection is inhibited by HCV receptor-specific antibodies, interferon, and specific antiviral agents. The observation that HCV-infected hCMEC/D3 cells release low levels of infectious virus and show evidence of apoptosis supports a model in which the BBB may provide an extrahepatic target for infection, and HCV may directly induce neuropathology *in vivo*.

Supplementary Material

Note: To access the supplementary material accompanying this article, visit the online version of *Gastroenterology* at www.gastrojournal.org, and at doi: 10.1053/j.gastro.2011.11.028.

References

1. Hoofnagle JH. Course and outcome of hepatitis C. *Hepatology* 2002;36:S21–S29.
2. Morgello S. The nervous system and hepatitis C virus. *Semin Liver Dis* 2005;25:118–121.
3. Weissenborn K, Tryc AB, Heeren M, et al. Hepatitis C virus infection and the brain. *Metab Brain Dis* 2009;24:197–210.
4. Radkowski M, Wilkinson J, Nowicki M, et al. Search for hepatitis C virus negative-strand RNA sequences and analysis of viral sequences in the central nervous system: evidence of replication. *J Virol* 2002;76:600–608.
5. Forton DM, Karayiannis P, Mahmud N, et al. Identification of unique hepatitis C virus quasispecies in the central nervous system and comparative analysis of internal translational efficiency of brain, liver, and serum variants. *J Virol* 2004;78:5170–5183.
6. Shimizu YK, Igarashi H, Kanematu T, et al. Sequence analysis of the hepatitis C virus genome recovered from serum, liver, and peripheral blood mononuclear cells of infected chimpanzees. *J Virol* 1997;71:5769–5773.
7. Burlone ME, Budkowska A. Hepatitis C virus cell entry: role of lipoproteins and cellular receptors. *J Gen Virol* 2009;90:1055–1070.
8. Jo J, Lohmann V, Bartenschlager R, et al. Experimental models to study the immunobiology of hepatitis C virus. *J Gen Virol* 2011;92:477–493.
9. Kato T, Date T, Miyamoto M, et al. Nonhepatic cell lines HeLa and 293 support efficient replication of the hepatitis C virus genotype 2a subgenomic replicon. *J Virol* 2005;79:592–596.
10. Fletcher NF, Yang JP, Farquhar MJ, et al. Hepatitis C virus infection of neuroepithelioma cell lines. *Gastroenterology* 2010;139:1365–1374 e2.
11. Stins MF, Badger J, Sik Kim K. Bacterial invasion and transcytosis in transfected human brain microvascular endothelial cells. *Microb Pathog* 2001;30:19–28.
12. Weksler BB, Subileau EA, Perriere N, et al. Blood-brain barrier-specific properties of a human adult brain endothelial cell line. *FASEB J* 2005;19:1872–1874.
13. Lalor PF, Edwards S, McNab G, et al. Vascular adhesion protein-1 mediates adhesion and transmigration of lymphocytes on human hepatic endothelial cells. *J Immunol* 2002;169:983–992.
14. Schwarz AK, Grove J, Hu K, et al. Hepatoma cell density promotes claudin-1 and scavenger receptor BI expression and hepatitis C virus internalization. *J Virol* 2009;83:12407–12414.
15. Krieger SE, Zeisel MB, Davis C, et al. Inhibition of hepatitis C virus infection by anti-claudin-1 antibodies is mediated by neutralization of E2-CD81-claudin-1 associations. *Hepatology* 2010;51:1144–1157.
16. Chang KS, Jiang J, Cai Z, et al. Human apolipoprotein e is required for infectivity and production of hepatitis C virus in cell culture. *J Virol* 2007;81:13783–13793.
17. Hsu M, Zhang J, Flint M, et al. Hepatitis C virus glycoproteins mediate pH-dependent cell entry of pseudotyped retroviral particles. *Proc Natl Acad Sci U S A* 2003;100:7271–7276.
18. Jensen TB, Gottwein JM, Scheel TK, et al. Highly efficient JFH1-based cell-culture system for hepatitis C virus genotype 5a: failure of homologous neutralizing-antibody treatment to control infection. *J Infect Dis* 2008;198:1756–1765.
19. Lindenbach BD, Evans MJ, Syder AJ, et al. Complete replication of hepatitis C virus in cell culture. *Science* 2005;309:623–626.
20. Poller B, Gutmann H, Krahenbuhl S, et al. The human brain endothelial cell line hCMEC/D3 as a human blood-brain barrier model for drug transport studies. *J Neurochem* 2008;107:1358–1368.
21. Dehouck MP, Jolliet-Riant P, Bree F, et al. Drug transfer across the blood-brain barrier: correlation between *in vitro* and *in vivo* models. *J Neurochem* 1992;58:1790–1797.
22. Murray J, Fishman SL, Ryan E, et al. Clinicopathologic correlates of hepatitis C virus in brain: a pilot study. *J Neurovirol* 2008;14:17–27.
23. Popescu CI, Dubuisson J. Role of lipid metabolism in hepatitis C virus assembly and entry. *Biol Cell* 2010;102:63–74.
24. Hishiki T, Shimizu Y, Tobita R, et al. Hepatitis C virus infectivity is influenced by association of apolipoprotein E isoforms. *J Virol* 2010;84:12048–12057.
25. Jopling CL, Yi M, Lancaster AM, et al. Modulation of hepatitis C virus RNA abundance by a liver-specific MicroRNA. *Science* 2005;309:1577–1581.
26. Deng L, Adachi T, Kitayama K, et al. Hepatitis C virus infection induces apoptosis through a Bax-triggered, mitochondrion-mediated, caspase 3-dependent pathway. *J Virol* 2008;82:10375–10385.
27. McAndrews MP, Farcnik K, Carlen P, et al. Prevalence and significance of neurocognitive dysfunction in hepatitis C in the absence of correlated risk factors. *Hepatology* 2005;41:801–808.
28. Ballabh P, Braun A, Nedergaard M. The blood-brain barrier: an overview: structure, regulation, and clinical implications. *Neurobiol Dis* 2004;16:1–13.

29. Fishman SL, Murray JM, Eng FJ, et al. Molecular and bioinformatic evidence of hepatitis C virus evolution in brain. *J Infect Dis* 2008; 197:597–607. 522
30. Lau DT, Fish PM, Sinha M, et al. Interferon regulatory factor-3 activation, hepatic interferon-stimulated gene expression, and immune cell infiltration in hepatitis C virus patients. *Hepatology* 2008;47:799–809. 523
31. Liang Y, Shilagard T, Xiao SY, et al. Visualizing hepatitis C virus infections in human liver by two-photon microscopy. *Gastroenterology* 2009;137:1448–1458. 524
32. Wilkinson J, Radkowski M, Laskus T. Hepatitis C virus neuroinvasion: identification of infected cells. *J Virol* 2009;83:1312–1319. 525
33. Vivithanaporn P, Maingat F, Lin LT, et al. Hepatitis C virus core protein induces neuroimmune activation and potentiates human immunodeficiency virus-1 neurotoxicity. *PLoS One* 2010; 5:e12856. 526
34. Farquhar MJ, McKeating JA. Primary hepatocytes as targets for hepatitis C virus replication. *J Viral Hepat* 2008;15:849–854. 527
35. Ploss A, Evans MJ, Gaysinskaya VA, et al. Human occludin is a hepatitis C virus entry factor required for infection of mouse cells. *Nature* 2009;457:882–886. 528
36. Su AI, Wiltshire T, Batalov S, et al. A gene atlas of the mouse and human protein-encoding transcriptomes. *Proc Natl Acad Sci U S A* 2004;101:6062–6067. 529
37. Berglund L, Bjorling E, Oksvold P, et al. A gene-centric Human Protein Atlas for expression profiles based on antibodies. *Mol Cell Proteomics* 2008;7:2019–2027. 530
38. Hulsermann U, Hoffmann MM, Massing U, et al. Uptake of apolipoprotein E fragment coupled liposomes by cultured brain microvessel endothelial cells and intact brain capillaries. *J Drug Target* 2009;17:610–618. 531
39. Zensi A, Begley D, Pontikis C, et al. Albumin nanoparticles targeted with Apo E enter the CNS by transcytosis and are delivered to neurones. *J Control Release* 2009;137:78–86. 532
40. Varatharajan L, Thomas SA. The transport of anti-HIV drugs across blood-CNS interfaces: summary of current knowledge and recommendations for further research. *Antiviral Res* 2009;82:A99–A109. 533
41. Kramer-Hammerle S, Rothenaigner I, Wolff H, et al. Cells of the central nervous system as targets and reservoirs of the human immunodeficiency virus. *Virus Res* 2005;111:194–213. 534
42. Diamond MS, Klein RS. West Nile virus: crossing the blood-brain barrier. *Nat Med* 2004;10:1294–1295. 535

Received June 18, 2011. Accepted November 15, 2011.

Reprint requests

Address requests for reprints to: Jane A. McKeating. e-mail: j.a.mckeating@bham.ac.uk; fax: (44) 121-414-3599.

Acknowledgments

The authors thank C. Rice for J6/JFH, Huh-7.5, and anti-NS5A 9E10; J. Bukh for SA13/JFH and T. Wakita for JFH-1; J. Neyts for anti-HCV compounds; S. Ray for HCVpp plasmids; and Colin Howard for critical reading of the manuscript.

Conflicts of interest

The authors disclose no conflicts.

Funding

Supported by grants from the MRC G0400802 and Wellcome Trust.

AQ: 1

AQ: 2

AQ: 3

AQ: 4

Supplementary Materials and Methods

Clinical Samples and RNA Preparation

Clinical samples for qRT-PCR and immunohistochemical analyses (Table 1, Figure 1, and Supplementary Figure 1) were obtained from the Manhattan HIV Brain Bank and Manhattan Hepatology Brain Bank (R24MH59724) or from the Mount Sinai Department of Pathology autopsy service under an institutional review board-approved protocol. Subjects enrolled in the Manhattan Hepatology Brain Bank are in advanced stages of HIV and liver disease and agree to be organ donors for the purposes of research upon their death. Plasma collection and cognitive assessments were performed on Manhattan Hepatology Brain Bank participants at regular intervals until death. The 10 subjects whose HCV RNA was analyzed were a subset of individuals with premortem evidence of active HCV infection (eg, plasma viremia). None had undergone HCV-targeted therapies between the time of HCV plasma load determination and death, with the exception of patient 40003, who received a 1-month course of interferon and ribavirin 3 months before death.¹ Eligibility criteria for the Manhattan HIV Brain Bank have been previously reported.² Briefly, patients must be HIV positive, consent to postmortem organ donation, and (1) have a condition indicative of advanced HIV disease or another disease without effective therapy, (2) have a CD4 cell count of no more than 50 cells/ μ L for at least 3 months, or (3) be at risk for near-term mortality in the judgment of the primary physician.

Samples of liver and brain material were stored at -80°C ; for RNA extraction, 10 mg tissue was removed and homogenized using sterile disposable plastic homogenizers. Instruments were changed between each sample to eliminate cross-contamination. RNA was extracted using the RNeasy Mini Kit (Qiagen) according to the manufacturer's instructions.

Northern Blotting for miR-122

RNA from Huh-7 or hCMEC/D3 cells was extracted using TRI Reagent (Sigma). Five micrograms of total RNA was separated by denaturing polyacrylamide gel electrophoresis on gels containing 15% polyacrylamide, 8 mol/L urea, and $0.5\times$ TBE (Tris-borate EDTA). RNA was transferred to Hybond NX membrane (GE Healthcare) using a semi-dry transfer apparatus and cross-linked to the membrane using EDC, as described in Pall and Hamilton.³ Membranes were probed overnight with γ -³²P adenosine triphosphate end-labeled DNA oligonucleotides complementary to miR-122 (5'-ACAAA-CACCATTGTCACTCCA-3') or a U6 small nuclear RNA control (5'-ATATGGAACGCTTCACGAATT-3'). Hybridization took place at 37°C in hybridization solution ($5\times$ SSPE, $7.5\times$ Denhardt's solution, 0.1% sodium dodecyl

sulfate) supplemented with 50 $\mu\text{g}/\text{mL}$ yeast transfer RNA. Membranes were washed twice in $5\times$ SSPE/0.1% sodium dodecyl sulfate at room temperature and twice in $1\times$ SSPE/0.1% sodium dodecyl sulfate at 37°C before visualization on a Storm 825 PhosphorImager (GE Healthcare).

qRT-PCR for miR-122

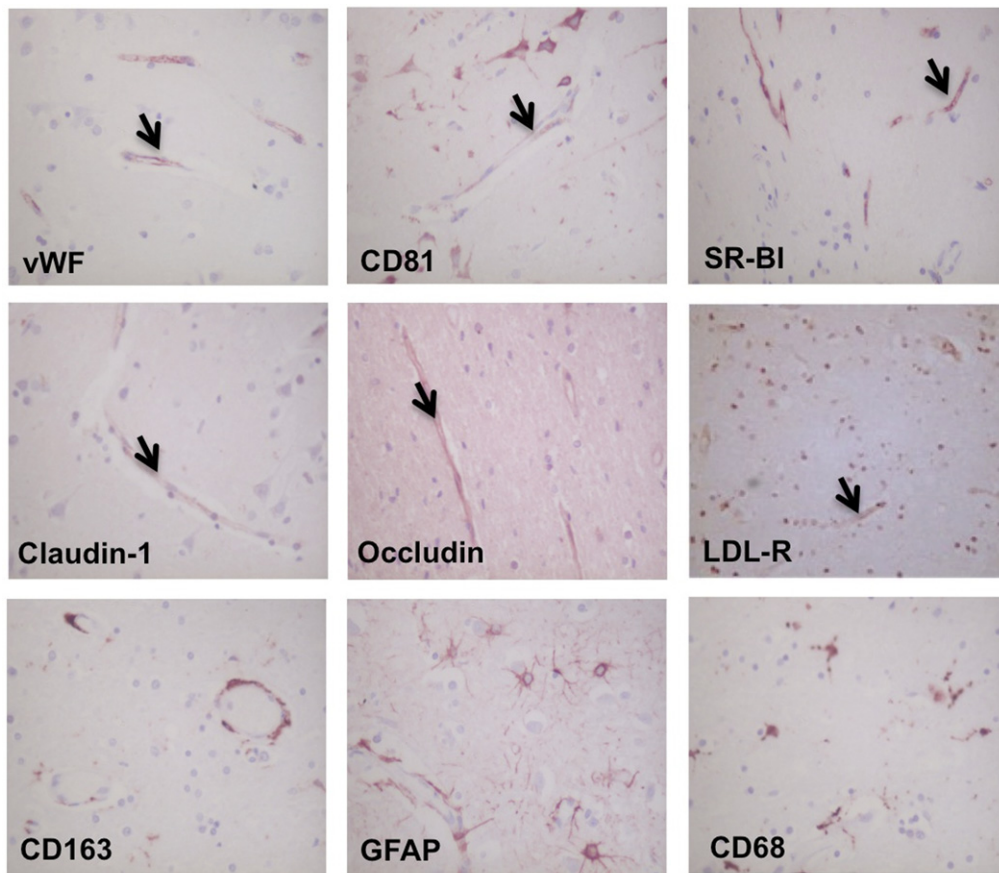
A total of 10 ng total RNA was analyzed by qRT-PCR by using TaqMan microRNA assays specific to miR-122 or a U6 small nuclear RNA control (Applied Biosystems), according to the manufacturer's instructions. Assays were performed in a Stratagene Mx3005P machine (Agilent Technologies) and miR-122 levels expressed relative to U6 levels by the $2^{-\Delta\Delta\text{Ct}}$ method. For comparison of different clinical samples, U6 levels varied considerably between different tissues so miR-122 levels were expressed as $2^{-\Delta\text{Ct}}$.

Transfection of hCMEC/D3 Cells With miR-122 Expression Vectors and HCVcc Infection

hCMEC/D3 cells were transfected with miR-122 wild-type duplex RNA or miR-122 p3+4 mutant duplex, using RNAiMax as described.⁴ Twenty-four hours after transfection, cells were infected with HCVcc SA13/JFH and duplicate wells were harvested for miR-122 expression by using qRT-PCR. After 72 hours, infected cells were stained with anti-NS5A antibody and visualized with an anti-mouse Alexa 594 antibody. Infected foci were enumerated and infection levels expressed as focus-forming units per milliliter. To confirm incorporation of miR-122 WT duplexes into a functional RNA-induced gene silencing complex, hCMEC/D3 cells were cotransfected with miR-122 duplex and a miR-122 sensor expressing either green fluorescent protein or firefly luciferase.⁵ Forty-eight hours after transfection, cells were fixed by using 1% paraformaldehyde and transfection efficiency quantified by using flow cytometry (green fluorescent protein constructs) or were lysed and luciferase activity quantified by using the Dual Luciferase Assay System (Promega).

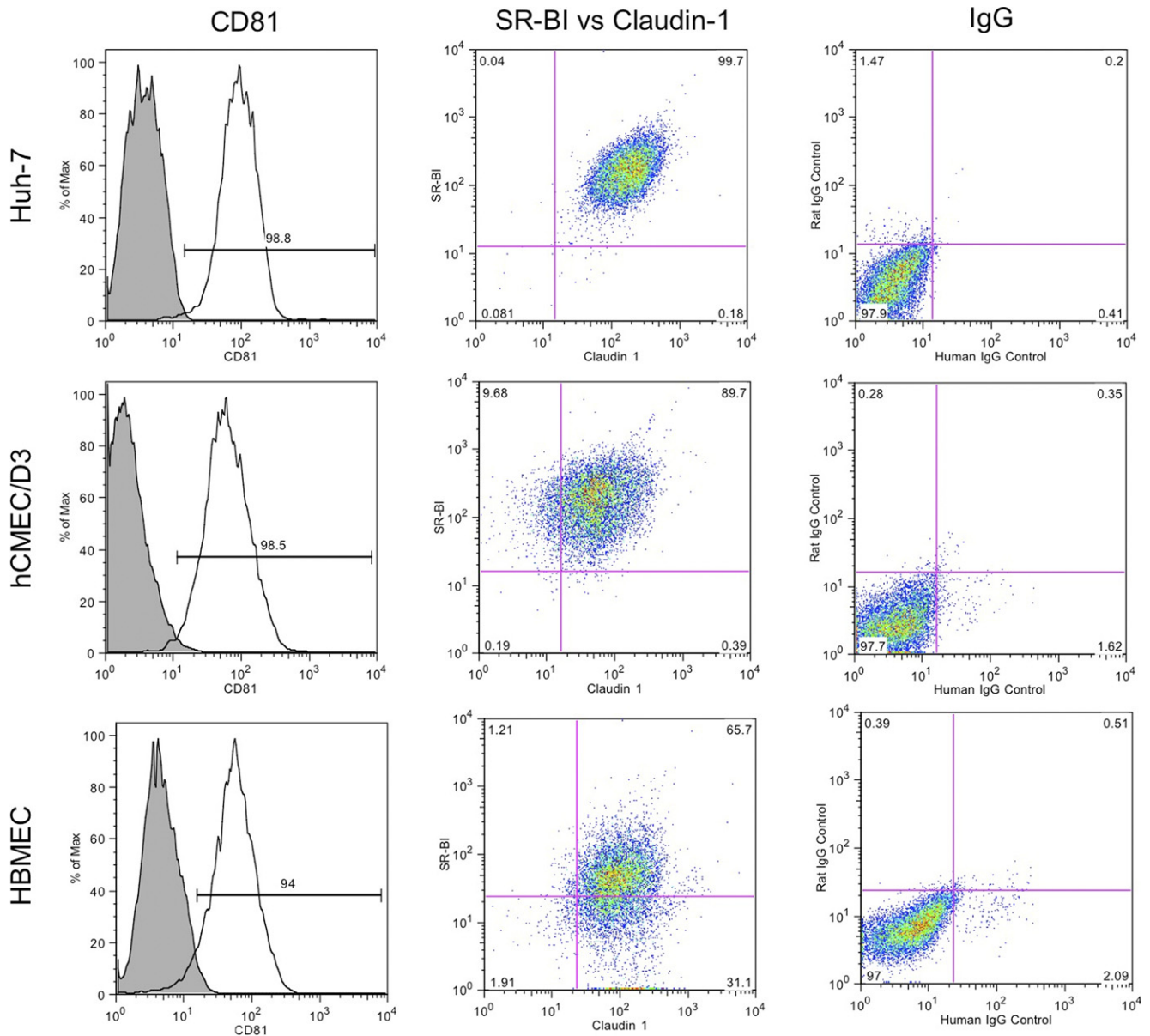
Supplementary References

- Murray J, Fishman SL, Ryan E, et al. Clinicopathologic correlates of hepatitis C virus in brain: a pilot study. *J Neurovirol* 2008; 14:17–27.
- Morgello S, Estanislao L, Simpson D, et al. HIV-associated distal sensory polyneuropathy in the era of highly active antiretroviral therapy: the Manhattan HIV Brain Bank. *Arch Neurol* 2004;61: 546–551.
- Pall GS, Hamilton AJ. Improved northern blot method for enhanced detection of small RNA. *Nat Protoc* 2008;3:1077–1084.
- Jopling CL, Yi M, Lancaster AM, et al. Modulation of hepatitis C virus RNA abundance by a liver-specific MicroRNA. *Science* 2005; 309:1577–1581.
- Roberts AP, Lewis AP, Jopling CL. miR-122 activates hepatitis C virus translation by a specialized mechanism requiring particular RNA components. *Nucleic Acids Res* 2011;39:7716–7729.

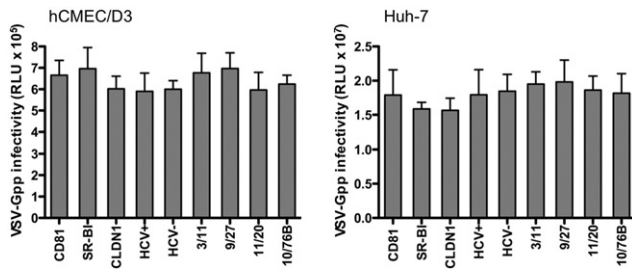


Supplementary Figure 1. Immunohistochemical staining of human brain tissue. Sections of formalin-fixed, paraffin-embedded human cerebral cortex were stained with antibodies to detect von Willebrand Factor (vWF; brain endothelium), together with the HCV entry factors CD81, SR-BI, claudin-1, occludin, and LDL-R. Arrows denote brain endothelium. Antibodies to detect CD163 (perivascular macrophages), glial fibrillary acidic protein (astrocytes), and CD68 (macrophages) show the localization of cell types in close proximity to brain endothelium. Original magnification 200X.

636
637
638
639
640
641
642
643
644
645
646
647
648
649
650
651
652
653
654
655
656
657
658
659
660
661
662
663
664
665
666
667
668
669
670
671
672
673
674
675
676
677
678
679
680
681
682
683
684
685
686
687
688
689
690
691



Supplementary Figure 2. Coexpression of HCV entry factors on permissive Huh-7 and brain endothelial cells. To investigate the percentage of brain endothelial cells that express all HCV entry factors, cells were costained for CD81, SR-BI, and claudin-1. Flow cytometry showed that >90% of cells expressed CD81 and occludin (Figure 2), and 99.7% of Huh-7 cells coexpressed SR-BI and claudin, with slightly lower levels of coexpression observed on hCMEC/D3 (89.7%) and HBMEC (65.7%). Anti-receptor antibodies showed negligible binding to receptor-negative Chinese hamster ovary cells with mean fluorescence intensity values between 5 and 11.

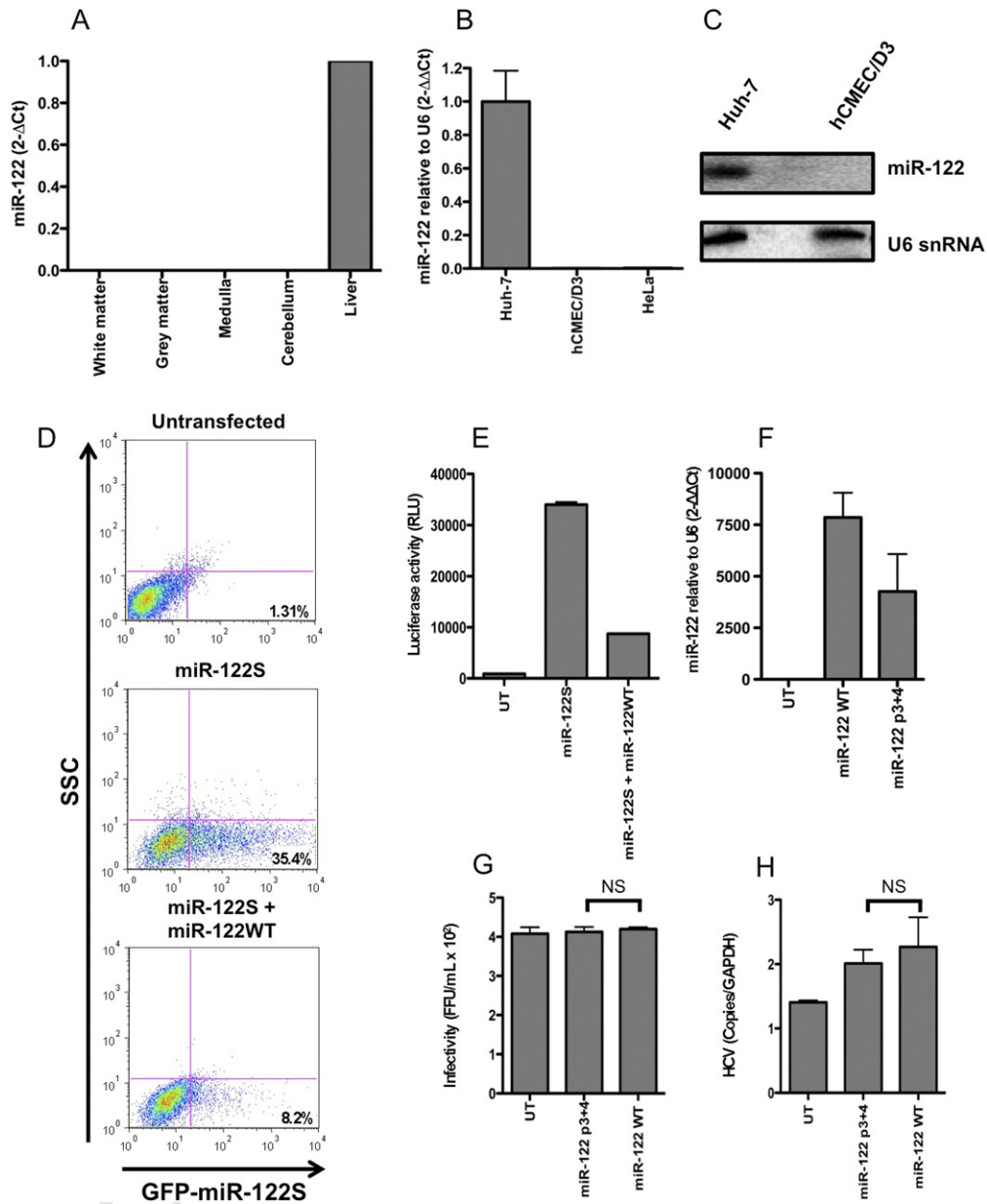


Supplementary Figure 3. Effect of neutralizing antibody on VSV-Gpp infection. hCMEC/D3 or Huh-7 cells were treated with 10 μ g of the indicated neutralizing antibodies for 1 hour and then infected with VSV-Gpp. After 72 hours, cells were lysed and infectivity measured and expressed as relative light units minus the no-envelope signal. There was no effect of any of the antibodies on VSV-Gpp infectivity.

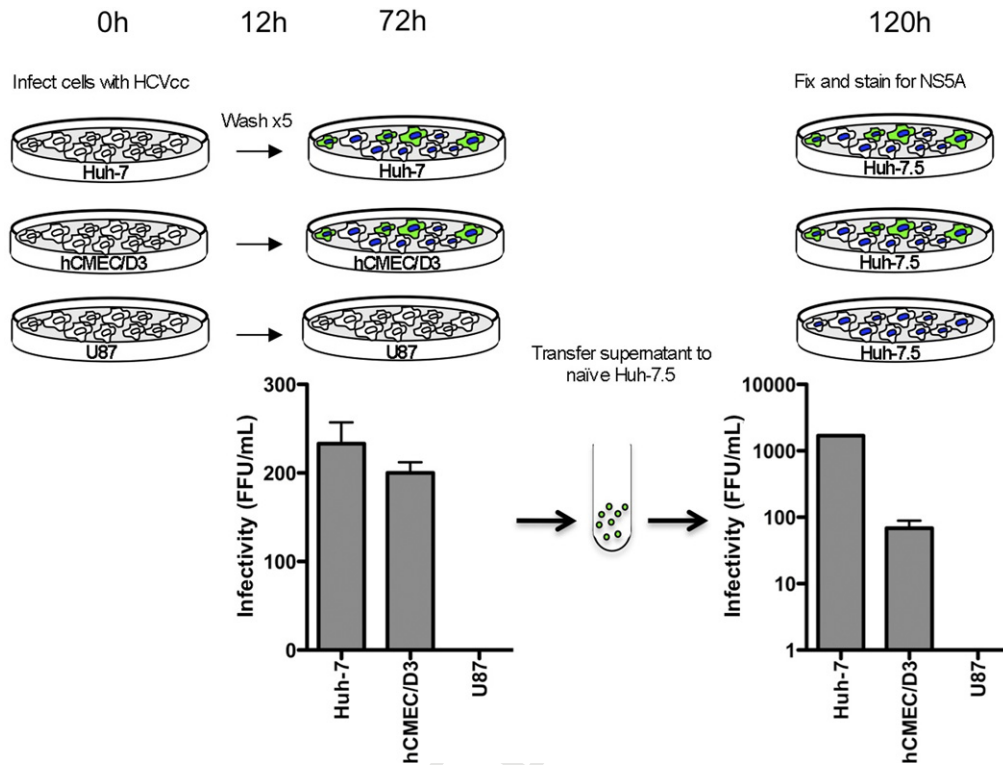
UNCORRECTED PROOF

748
749
750
751
752
753
754
755
756
757
758
759
760
761
762
763
764
765
766
767
768
769
770
771
772
773
774
775
776
777
778
779
780
781
782
783
784
785
786
787
788
789
790
791
792
793
794
795
796
797
798
799
800
801
802
803

748
749
750
751
752
753
754
755
756
757
758
759
760
761
762
763
764
765
766
767
768
769
770
771
772
773
774
775
776
777
778
779
780
781
782
783
784
785
786
787
788
789
790
791
792
793
794
795
796
797
798
799
800
801
802
803



Supplementary Figure 4. miR-122 expression on brain tissue and hCMEC/D3 cells. Total RNA extracted from the brain and liver tissue from 3 HCV-seropositive subjects was analyzed by qPCR for miR-122. miR-122 levels are shown as 2^{-ΔCt} relative to liver as an average ± SD of 3 subjects. (A) Total RNA was extracted from Huh-7, hCMEC/D3, or HeLa cells. miR-122 levels were determined relative to a U6 small nuclear RNA control by qRT-PCR, and data are shown as 2^{-ΔΔCt} relative to Huh-7 cells as an average ± SD of triplicate samples. (B) Although Huh-7 cells express high levels of miR-122, hCMEC/D3 cells did not express detectable levels of miR-122. (C) Northern blot analysis confirmed miR-122 expression in Huh-7 but not hCMEC/D3 cells. hCMEC/D3 cells were transfected with miR-122 sensor (miR-122S) expressing green fluorescent protein with a complementary target site for miR-122 in the presence or absence of miR-122 duplex. (D) Flow cytometry revealed 35% of cells expressing miR-122 green fluorescent protein sensor that was significantly reduced following transfection of miR-122, confirming miR-122 incorporation into a functional RNA-induced gene silencing complex. (E) Flow cytometry data was confirmed using a miR-122 sensor expressing firefly luciferase. (F) miR-122 expression was confirmed by qPCR as in C, with data shown relative to untransfected cells. (G and H) HCVcc infection levels and HCV RNA levels were not significantly increased compared with controls following miR-122 WT or miR-122 p3+4 mutant expression in hCMEC/D3 cells.



Supplementary Figure 5. HCV-infected brain endothelial cells release infectious virus. hCMEC/D3, Huh-7, or the nonpermissive U87 cell line was infected with HCVcc SA13/JFH at equivalent multiplicities of infection. After 12 hours, input virus was removed by extensive washing. Cells were incubated at 37°C for 72 hours, and extracellular medium was collected and used to inoculate naïve Huh-7.5 cells. The level of infectious virus released from hCMEC/D3 over an 8-hour period was approximately 10-fold lower than that released from Huh-7 cells. No infectious virus was detected in the medium from nonpermissive U87 cells. Furthermore, medium collected after 12 hours contained no detectable virus, showing that brain endothelial cells release low levels of HCV that is infectious for Huh-7 hepatoma cells.